Electronic Supplementary Information

A tetrahedral DNA nanorobot with conformational change in response to molecular trigger

Fengyu Liu,[a] Xiaoming Liu,*[a] Qing Shi,[a] Christopher Maffeo,[b] Masaru Kojima,[c] Lixin Dong,[d] Aleksei Aksimentiev,[b] Qiang Huang,[a] Toshio Fukuda[a] and Tatsuo Arai[a]

[a] Key Laboratory of Biomimetic Robots and Systems, Ministry of Education, State Key Laboratory of Intelligent Control and Decision of Complex System, Beijing Advanced Innovation Center for Intelligent Robots and Systems and School of Mechatronical Engineering, Beijing Institute of Technology, Beijing 100081, China.

[b] Department of Physics, University of Illinois at Urbana Champaign, Urbana IL 61802, USA.

[c] Department of Materials Engineering Science, Osaka University, Osaka 560-8531, Japan.

[d] Department of Biomedical Engineering, City University of Hong Kong, Hong Kong 999077, China.

Corresponding Author

*Email: liuxiaoming555@bit.edu.cn.

This Electronic Supplementary Information PDF includes:

Experimental Section

Multiresolution Simulations

The simulations of the tetrahedral nanostructure were first performed using the mrdna framework.[5] A script was used to import the cadnano[1] design into the framework, to fold it by 90 degrees along each designed folding axes, and to hybridize the lock strands. The multiresolution simulation was performed in three stages as previously described.[5] Briefly, a 4 bp/bead model of the nanostructure was generated and used in a 20 μs simulation to reveal the fluctuations of the structure, assuming the self-assembly occurred as designed. The nanostructure configuration at the end of the simulation was used to update splines representing the centerline of each helix. Subsequently, a higher resolution 2 bead/bp model with an explicit, local representation of the twist in each helix was generated and relaxed during a 400 ns simulation. During this simulation, the twist dihedral angle potential was smoothly truncated so that the linking number between crossovers could relax. The configuration from the last 5 ns of the simulation was averaged and used to update the configuration of the beads for the final 400 ns simulation with the linking number of each helix held fixed by harmonic twist dihedral angle potentials. The configuration of the object at the end of the final mrdna simulation was mapped into an oxDNA2[2-4] model using the mrdna package. After 500 steps of minimization, the oxDNA model was simulated for over 750 ns. The tacoxDNA[6] package was used to process the oxDNA trajectory for visualization and analysis. Base pairs were considered intact when the bases fell within a 5 Å cutoff VMD[7] was used to visualize all simulations.

Cell Culture

The HT29 human colon cancer cell line and the BJ skin fibroblast cell line were obtained from the American Type Culture Collection (ATCC, USA) and cultured in Dulbecco's modified Eagle's medium (DMEM) supplemented with 10% fetal bovine serum (Gibco, USA), 100 U/mL penicillin, and 100 μg/mL streptomycin. All cells should be kept in humidified air containing 5% CO_2 at 37 °C.

Preparation of Various Nanostructures

For DOS: 2 μg of M13mp18 single-stranded DNA (NEB, UK) was cleaved by restriction endonucleases *Bsp1286 I* (2 U/μL) and *Kpn I* (2 U/μL), supplemented with two help strands (1 μM) in 1× CutSmart Buffer. The reaction was carried out at 37 °C for 4 h. The target fragments of the p1498 were then recovered using a gel extraction kit (Thermo Fisher, USA). Based on the sequences derived from caDNAno[1], multiple staple strands mixed with p1498 at a concentration ratio of 1:10 then reacted in the reaction buffer (containing 10 mM Tris, 1 mM EDTA, and 10 mM $MgCl_2$) for more than 10 h. The assembly reaction was performed by incubating the mixed solution at 95 °C for 30 s, followed by a temperature decrease of 1 °C / min until 65 °C, and afterward a decrease of 1 °C /10 min until 20 °C. After that, the mixed solution was passed

through Amicon Ultra-0.5 ml 100 kD centrifugal filters (Millipore Corporation, USA) three times at 2500 rpm to remove excess staple strands and harvest the purified DOS. Each ultrafiltration time did not exceed 3 min.

For BDT: Five random duplexes were synthesized (Table S1). These duplexes were then mixed with DOS at a molar ratio of 20:1. The folding reaction was performed at 40 °C for 10 min and then cooled to 20 °C at a 1 °C /10 min rate. The obtained BDT was rinsed three times at 2500 rpm through centrifugal filters to remove excess random duplexes.

For TDN: Firstly, five SYL3C aptamer duplexes (complementary length: 17 bp) were synthesized. These duplexes were then mixed with DOS at a molar ratio of 20: 1. For the folding reaction, the temperature was decreased from 40 °C to 20 °C at a rate of 1 °C /10 min. The mixture was rinsed three times with ultrafiltration tubes at 2500 rpm to harvest TDN. Each ultrafiltration time did not exceed 3 min.

Atomic Force Microscopy

Briefly, the purified sample (DOS) solution was deposited onto the surface of freshly cleaved mica, allowed to absorb 10 min, washed three times with distilled water, and then blown dry with nitrogen. AFM images of the DOS were acquired on a Park NX12 AFM (Park Systems, South Korea). For TDN, the sample solution was dropped on the new mica pieces and incubated at room temperature for 10 min. The mica pieces were then placed on the AFM bench, and the samples were scanned in a non-contact mode in liquid.

Confocal Microscopy

In a typical experiment, HT29 cells alone or BJ/HT29 co-cultures were grown overnight in 35 mm confocal dishes (Corning, USA) after inoculating. When the cell density reached 80%, 1 nM of a nanostructure (BDT or TDN) or free dye controls (FTR or FFD) was added to 1 ml of complete DMEM medium. After cultivation for 1 h in a 5% carbon dioxide incubator (Panasonic, Japan), cells were fixed with 4% paraformaldehyde for 10 min at room temperature, then washed three times with phosphate-buffered solution (PBS). The cell nuclei were stained by DAPI (4′, 6′-diamidino-2-phenylindole). Fluorescence images were captured using a confocal microscope (Nikon C2, Japan). *ImageJ* was applied to perform image analysis.

Flow Cytometry

HT29 cells and BJ cells were separately seeded on 24-well plates at a density of 5×10^5 cells/mL and cultured for 24 h. Then washed three times with PBS and incubated with Texas Red labeled TDN for 1 h at 37 °C. After incubation, cells were harvested and washed three times with PBS. The fluorescence intensity of the cells was determined by flow cytometry (BD Biosciences, USA).

Opened Efficiency Assay

To synthesize duplexes of different complementary lengths, as described in Table S2, we added 4 μM mixture of A1 into compA1-13bp(A3), compA1-17bp (A3), compA1-22bp (A3), or compA1-29bp(A3) and heat-shocked at 95 °C for 30 s then cooled to 20 °C at a rate of 1 min/°C. HT29 (2×10^5 cells/well) cells were seeded in 12-well plates and cultured for 24 h. Four types of duplexes were diluted in PBS to a 2 μM and added to the cell cultures. Cells treated with A1 were used as positive control. To rule out the possibility that duplexes were opened upon non-specific binding (false positive), we pretreated HT29 cells with 20 μg/ml antibodies against human EpCAM (Abcam, USA) before adding the duplexes. The fluorescence intensity was measured after 0, 0.5, 1, and 2 h by a fluorescence spectrometer (BioTek, USA).

Cell Viability Assay

According to the manufacturer's instructions, cell viability was evaluated using the Cell Counting Kit-8 (CCK-8) (Sigma-Aldrich, USA). Briefly, HT29 or BJ (5,000 cells/well) cells were seeded in 96-well plates and incubated overnight at 37 °C. To estimate the inherent cytotoxicity of TDN, various concentrations (0, 0.125, 0.25, 0.5, or 1 nM) of TDN were incubated with HT29 cells or BJ cells for 24 h. Wells with culture media and PBS were used as the blank and negative control, respectively. For viability measurements, CCK-8 (10 μL) was added to each well and incubated for 4 h, and then, the absorbance was measured at 450 nm (BioTek, USA).

Statistical Analysis

All experiments were independently repeated at least three times. Data are represented as the mean ± the standard deviation (SD). Unpaired student's *t*-tests were used to compare the means of two groups. One-way or two-way ANOVA was used to evaluate the statistical significance of the differences among the different groups. When ANOVA was significant, post hoc testing of differences between groups was performed using Dunnett's multiple comparisons test. All data were analyzed using GraphPad Prism 8.0 (GraphPad Software, USA). $*p < 0.05$ was considered statistically significant.

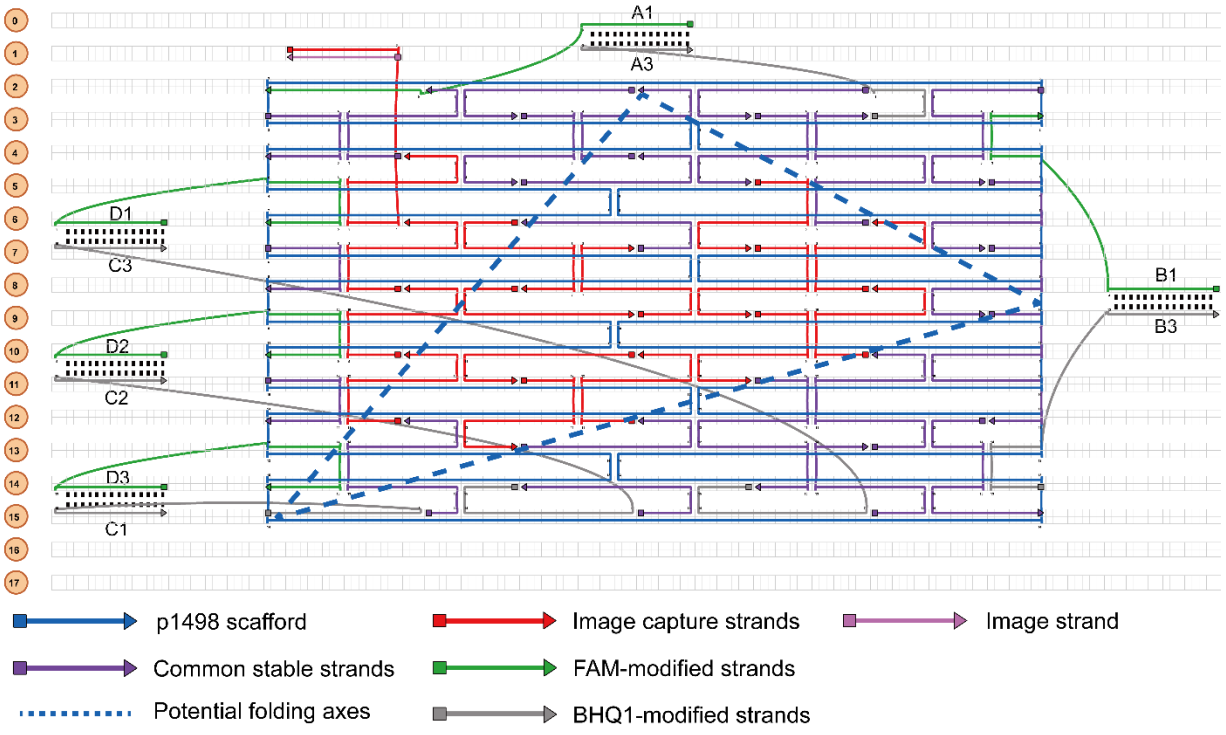

Figure S1. Design diagram of multiple nanostructures in caDNAno[1]. The essential elements for assembling DOS include common staple strands (purple), image capture strands (red), and p1498 scaffold (blue). The 3'end of the image strand is equipped with Texas red. All image capture strands (red) are extended at their 5'end to capture the image strands (pink). To keep the diagram clear, only a set of capture relationships between the image strand and image capture strand are shown here. Driven by hydrogen bonding between the five random duplexes (green, gray), DOS folds into BDT along three potential folding axes (blue dotted lines). Using SYL3C aptamer duplexes instead of random duplexes, DOS can be folded into controllable TDN through the same folding strategy as BDT. DOS can be converted to the targeted DOS(TDOS) by loading the SYL3C aptamer strands/random strands marked with the 6'FAM/BHQ1.

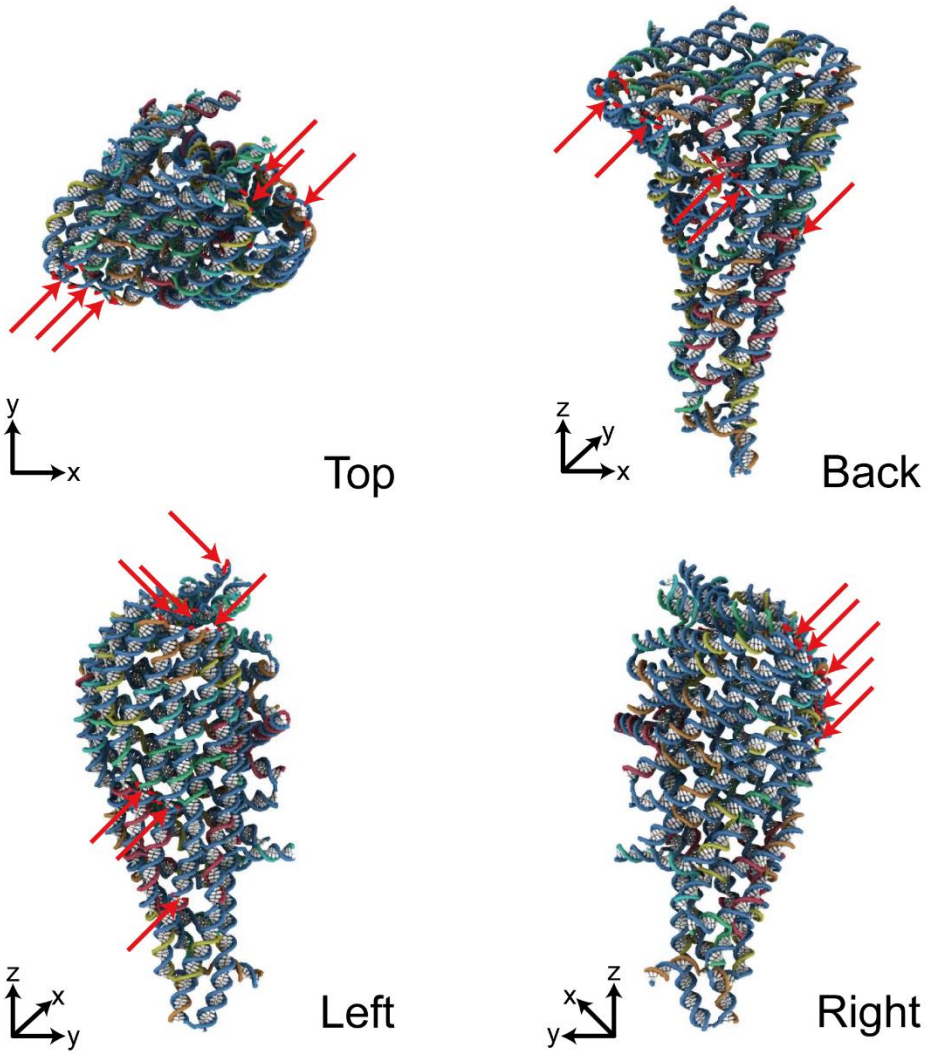

Figure S2. Multi-angle configuration of the tetrahedral object during oxDNA[2-4] simulations. These red arrows point to where the base pairs are broken. Similar simulation outcomes were observed in three independent runs.

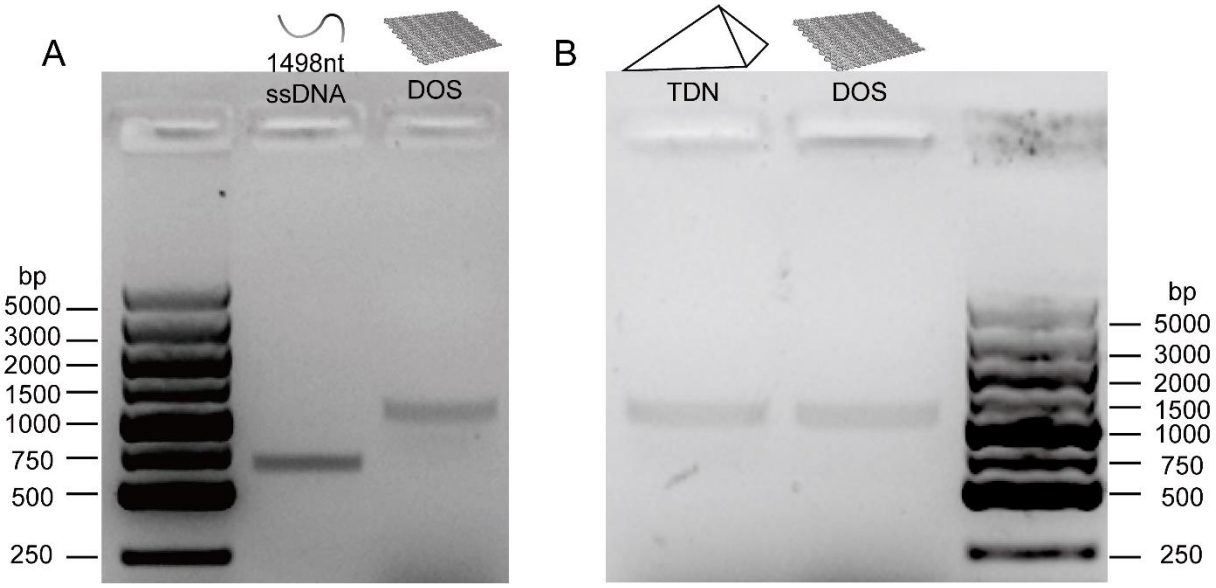

Figure S3. Characterization of DOS and TDN by gel electrophoresis. (A) The 1498nt single-stranded DNA (p1498) and DOS show different mobility in agarose gel (1% TAE). (B) The separation of DOS and TDN in agarose gel (1% TAE). The initial molar concentration of lane 1 and lane 2 are both 1 nM. The loading volume of lane 1 and lane 2 are both 30 μL. All data are representative of three independent experiments.

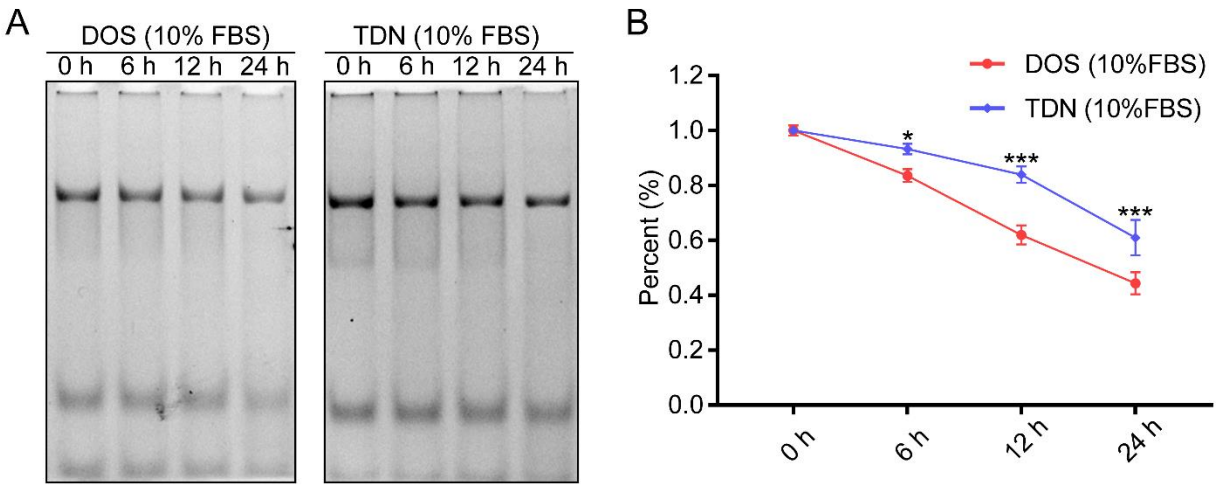

Figure S4. Serum stability of different nanostructures. (A) The equimolar concentration of TDN or DOS was incubated with cell culture medium (10% FBS) under physiological environment (pH 7.4, 37 °C) for 0h, 6h, 12h and 24h. The gels formula is 6% PAGE (1XTBE). (B) The degradation of DOS and TDN in cell culture medium (10% FBS). The data are representative of three independent experiments. *$p < 0.05$; ***$p < 0.001$.

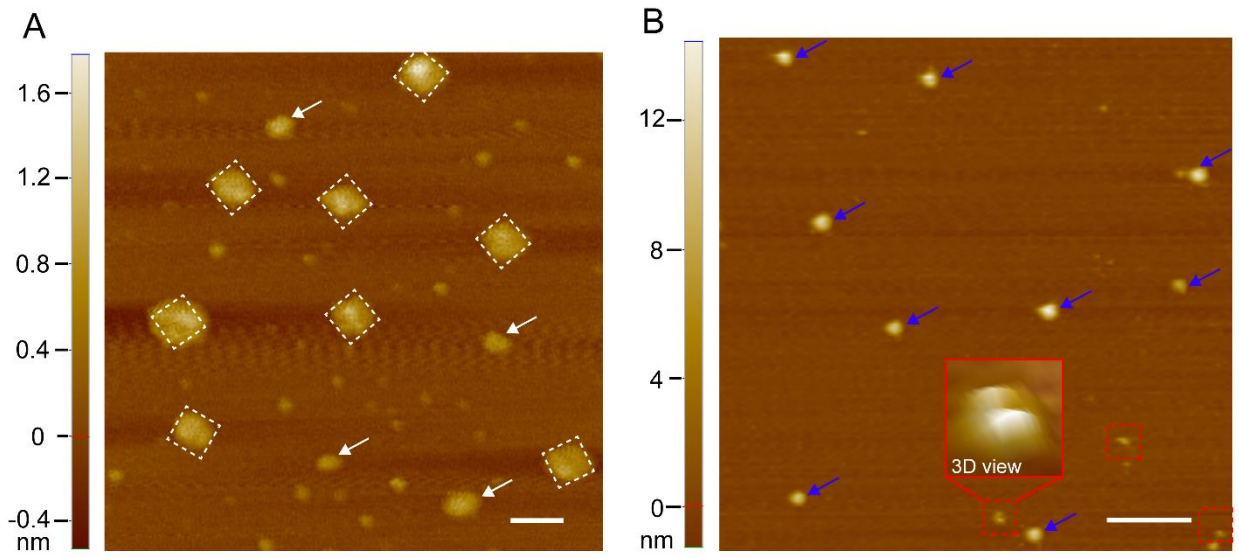

Figure S5. AFM characterizes the serum stability of TDN and DOS. (A) The degradation of DOS after treatment (37 °C, 12 h) with cell culture medium (10% FBS). The white dotted frames represent relatively complete DOS, and the white arrows point to fragments of DOS. Scale bar: 50 nm. (B) The morphology of TDN after incubation (37 °C, 12 h) in cell culture medium (10% FBS). The blue arrows refer to the intact tetrahedrons, and the red dotted frames represent the decomposed shapes. Scale bar: 100 nm. All data are representative of three independent experiments.

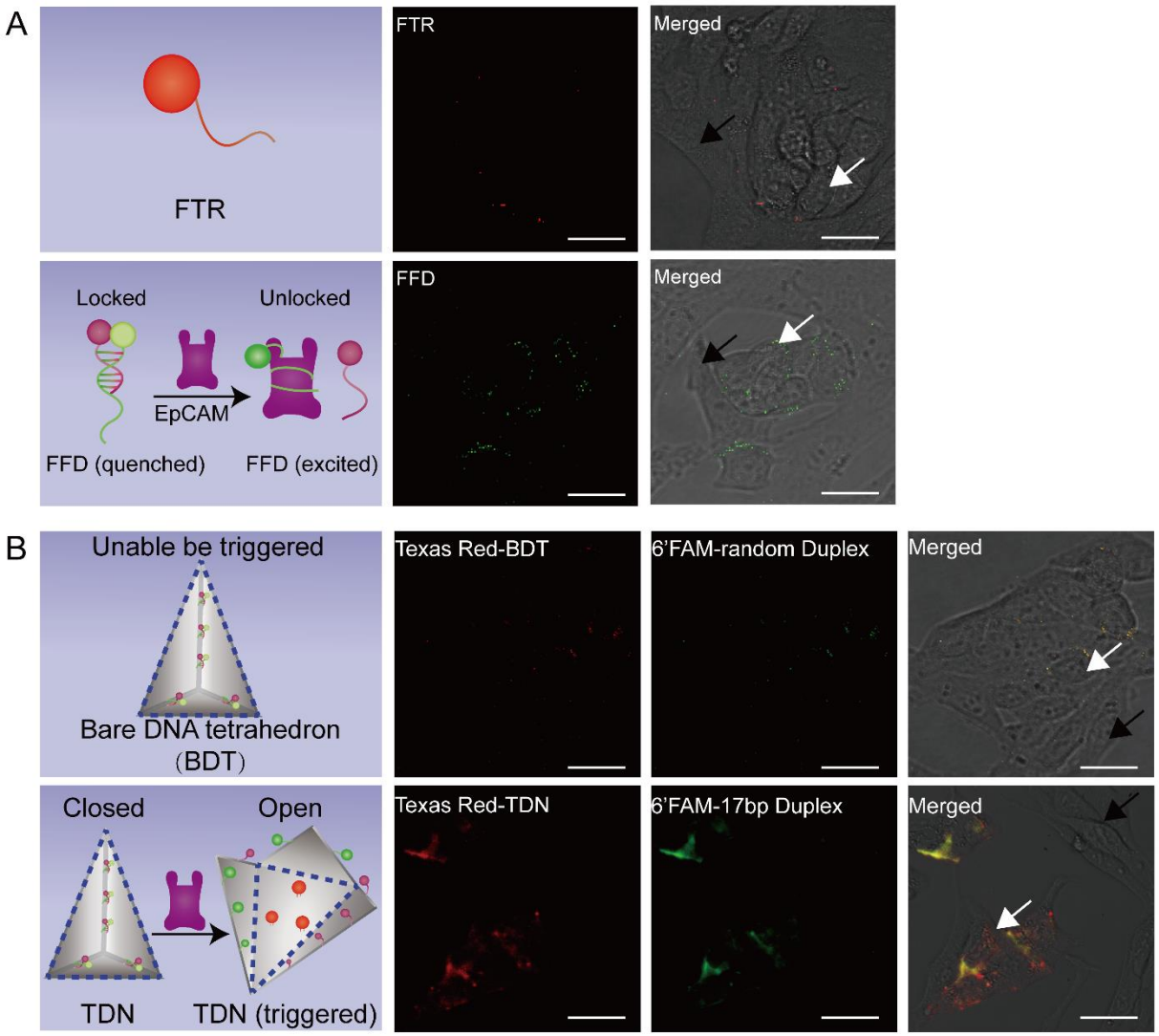

Figure S6. Confocal images of TDN specifically targeting HT29 cells in a co-culture model. (A) Negative and positive control results of co-cultured cell models. The upper and lower rows of co-cultured cell models were treated with FTR, and FFD, respectively. After incubation for 1 h at 37 °C, confocal images were obtained. The concentrations of FTR and FFD were all 1 nM. The white arrows refer to HT29 cells, and the black arrows point to BJ cells. The data are representative of three independent experiments. Scale Bars: 15 μm. (B) After incubating BDT (1 nM) and TDN (1 nM) in the co-cultured cell models for 1 h at 37 °C, confocal images were obtained. The white arrows refer to HT29 cells, and the black arrows point to BJ cells. The BDT and TDN were visualized with Texas Red. BDT's random duplexes and TDN's SYL3C aptamer duplexes were modified with 6'FAM. These images are representative of three independent experiments. Scale bars: 15 μm.

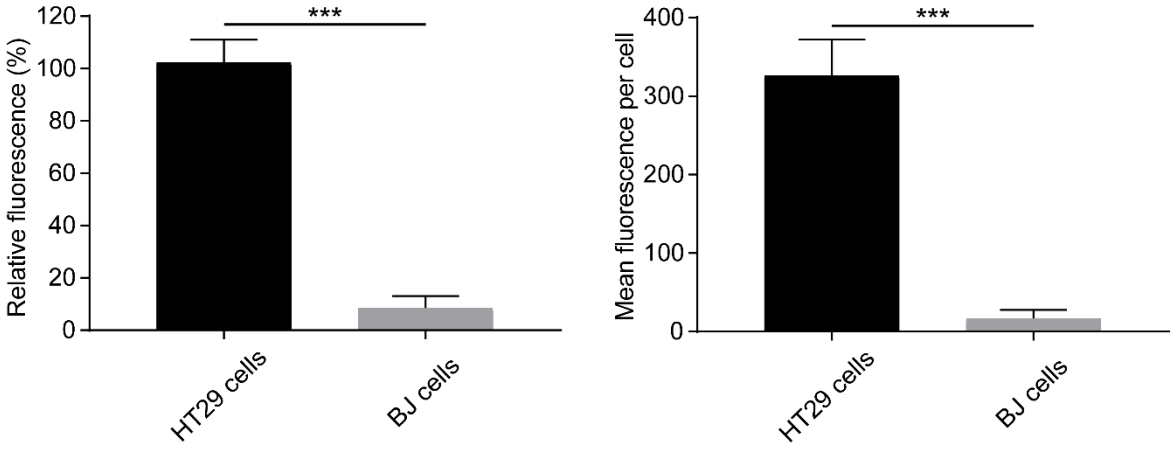

Figure S7. Flow cytometry analysis of cell uptake efficiency of TDN in HT29 cells or BJ cells. Data represent the mean ± SD of three independent experiments. Comparisons were made using the Student's t-test. ***$p < 0.001$.

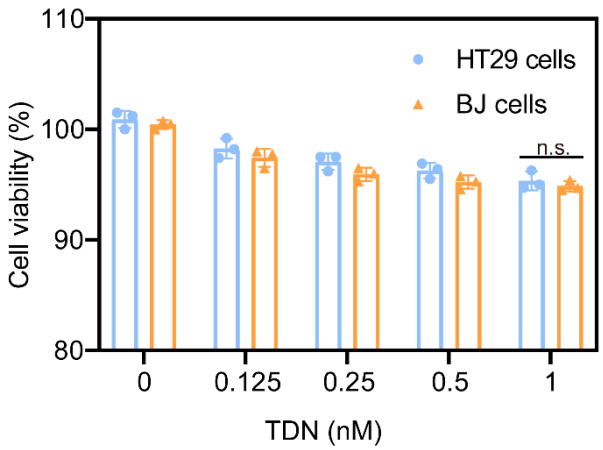

Figure S8. The result of cell viability to verify the low cytotoxicity of TDN. HT29 and BJ cells were treated with TDN (0, 0.125, 0.25, 0.5, or 1 nM) for 24 h at 37 °C. The cell viability was evaluated using a CCK-8 kit. Data represent the mean ± SD of three independent experiments. Comparisons were made using the Student's t-test. n.s. not significant.

Table S1. Detailed sequences of common staple strands and various functional strands.

Staple strands	
S1	AGTTGAAAGGAATTGAAAACCCTC
S2	GCTATTAGTCTCACCGCCTGCA
S3	TGATTAGTAATAAAAATCAAGTTTGCCAGAAT
S4	GTTCCGAAATCGTGAGACGGGC
S5	ACTAAATCTGACGGGGAAAGCCGGAAAGGAGCGGGCGCTAGTAACCAC
S6	CATCACGCAAACTTGCTGGTAA
S7	AAGTGTAACTCGAATTCGTAATCA
S8	TATCTTTAGTACCGAGAGCCTGGG
S9	GGAAACCTGTCGTGCCGCCC
S10	CCCTAAAGGGAGACGTCAAAGG
S11	TATCCAGAACATCACCAGTCAC
S12	AACAGCTTTTTCTTTTCACCAG
S13	GTGCCTTGCTGAACCTCAAATATCGGAAGGTTATCTAAAA
S14	TGGTCATAGCTGTTTCCACAACAT
S15	AGGGATTTGTGTTTTTATAATCAGTACTTCTT
S16	CAGCAGGCCCTGGCCCTGAGAGAGAGAGGCGGTTTGCGTACGGCCAAC
S17	GAATCAGAGCGAAGAGTCTGTC
S18	GCGAAAAAGAACGTGGACTCCA
S19	ACAGTGCCACGTCTGGTCAGTTGGCAAATCAAC
S20	ATTCCACTGTGTGAAATTGTTA
S21	CCTGAGAATAGACAGGAACGGTACGCTACAGG
S22	AAATACCTAACCATCACCCCATCACTTGCCTG
S23	CCGAGTAAGGAGCTAAACAGGAGGAGCACGTA
S24	ACGAGCCGTTGCGTTGCGCTCACTAGCTGCATTAATGAATTTGGGCGC
S25	ATCTAAAGCATCACCTAATGAGTGACGAACCA
S26	GCTTTCCAGTCGTCCGCTCACA
S27	AGAAAGCGCGAACGTGGCGAGAAATTTGGGGT
S28	AATCAATACTGAGAGCCAGCAGCAAGGCGGTC
S29	ACGACCAGTAAATTTTTGAATG
S30	TAACGTGCTTTCCTCGTTA
S31	GCGCGGGGAGCTAACTCACATTAAGAAGCATA
S32	CACACCCGCCGCGCTTAATGCGCCGGAAGGGA
S33	CCCCCGATTTAGAGCTGGAA
S34	GCGCGTACTATGGTTGCTTTGACGCCGATTAA
S35	GCAAAATCCCTTATAAGGTG
S36	GCGGTCACGCTGCGCGGGCGCTGGCAAGTGT
Help strands	
HS1	TCTTTAGGAGCACTAACAAC
HS2	AGGATCCCCGGGTACCGAG

Image capture strands	
TR1	GTGCGCAAAGAGTTTAAGCCTGACCTGAAAGCGTAAGAATTAGCCCTA
TR2	GTGCGCAAAGAGTTTACCAGCAGACCATTAAAAATACCGATTGCAGCA
TR3	GTGCGCAAAGAGTTTACGAGGTGCGATGGCCCACTACGTGTTGTTCCA
TR4	GTGCGCAAAGAGTTTATGTTTGATATCAAAAGAATAGCCCCAAGAGTC
TR5	GTGCGCAAAGAGTTTACAGACAATTAAAAGGGACATTCTGATTTACAT
TR6	GTGCGCAAAGAGTTTACTATCGGCTTAACCGTTGTAGCAATGAGGCCA
TR7	GTGCGCAAAGAGTTTACAGGGTGGTGATTGCCCTTCACCGGAAAATCC
TR8	GTGCGCAAAGAGTTTAAGTATTAATTAATGCGCGAACTGAACGTGGCA
TR9	GTGCGCAAAGAGTTTATGGCAGATATATTACCGCCAGCCAAACTCAAA
TR10	GTGCGCAAAGAGTTTAAAACATCGAGATAAAACAGAGGTGAATGAAAA
TR11	GTGCGCAAAGAGTTTAAATGGATTGCCAACAGAGATAGAACCCTTGGT
TR12	GTGCGCAAAGAGTTTAGTTTGGAAGAGATAGGGTTGAGTGGTTTGCCC
TR13	GTGCGCAAAGAGTTTACACTATTAAACCGTCTATCAGGGCCGTAAAGC
TR14	GTGCGCAAAGAGTTTAAGTAGAAGTTGCAACAGGAAAAACTCGTCTGA
TR15	GTGCGCAAAGAGTTTACCACGCTGACATTTTGACGCTCAAGCTCATGG
Image strand	
5' TAAACTCTTTGCGCAC 3' Texas red	
Random duplexes	
C1	ATAATGCTAGCAGTCCTTTAATAGACCTGGAATTGAAAACCCTC
D3	CCGTGACAAGGTCTATTAAAGGACTGCTAGCATTAT
D2	ATAATGCTAGCAGTCCTTTAATAGACCTTAAATTTTTGAATG
C2	ATTTCTATAGGTCTATTAAAGGACTGCTAGCATTAT
C3	ATAATGCTAGCAGTCCTTTAATAGACCTGCTGTTTCCACAACAT
D1	CGCACTACAGGTCTATTAAAGGACTGCTAGCATTAT
A1	ATAATGCTAGCAGTCCTTTAATAGACCTTTTCCTCGTTA
A3	GCCCACACAGGTCTATTAAAGGACTGCTAGCATTAT
B3	ATAATGCTAGCAGTCCTTTAATAGACCTGTCGTGCCGCCC
B1	TAGCCCCCAGGTCTATTAAAGGACTGCTAGCATTAT
SYL3C aptamer duplexes	
SYL3C: CACTACAGAGGTTGCGTCTGTCCCACGTTGTCATGGGGGGTTGGCCTG	
C1	CACTACAGAGGTTGCGTCTGTCCCACGTTGTCATGGGGGGTTGGCCTGGGAATTGAAAACCCTC
D3	CCGTGACATTTTTTTTTTTTTTTTTTTTTTTTTTTTTTTTACGCAACCTCTGTAGTG
D2	CACTACAGAGGTTGCGTCTGTCCCACGTTGTCATGGGGGGTTGGCCTGTAAATTTTTGAATG
C2	ATTTCTATTTTTTTTTTTTTTTTTTTTTTTTTTTTTTTTTTACGCAACCTCTGTAGTG
C3	CACTACAGAGGTTGCGTCTGTCCCACGTTGTCATGGGGGGTTGGCCTGGCTGTTTCCACAACAT
D1	CGCACTACTTTTTTTTTTTTTTTTTTTTTTTTTTTTTTTTTACGCAACCTCTGTAGTG
A1	CACTACAGAGGTTGCGTCTGTCCCACGTTGTCATGGGGGGTTGGCCTGTTTCCTCGTTA
A3	GCCCACACTTTTTTTTTTTTTTTTTTTTTTTTTTTTTTTTTACGCAACCTCTGTAGTG
B3	CACTACAGAGGTTGCGTCTGTCCCACGTTGTCATGGGGGGTTGGCCTGGTCGTGCCGCCC

B1	TAGCCCCCTTTTTTTTTTTTTTTTTTTTTTTTTTTTTTTTTTACGCAACCTCTGTAGTG

Duplexes design

Duplex 1: 5’ -6’FAM-C1- 3’; 5’ -D3-BHQ1- 3’

Duplex 2: 5’ -6’FAM-D2- 3’; 5’ -C2-BHQ1- 3’

Duplex 3: 5’ -6’FAM-C3- 3’; 5’ -D1-BHQ1- 3’

Duplex 4: 5’ -6’FAM-A1- 3’; 5’ -A3-BHQ1- 3’

Duplex 5: 5’ -6’FAM-B3- 3’; 5’ -B1-BHQ1- 3’

Table S2. Designed sequences for the duplex containing the SYL3C aptamer.

Name	Sequence (5'-3')	Modification
A1	CACTACAGAGGTTGCGTCTGTCCCACGTTGTCATGGGGG GTTGGCCTGTTTCCTCGTTA	5'-6'FAM
compA1-13bp(A3)	GCCCACACTTTTTTTTTTTTTTTTTTTTTTTTTTTTTTT AACCTCTGTAGTG	3'-BHQ1
compA1-17bp(A3)	GCCCACACTTTTTTTTTTTTTTTTTTTTTTTTTTTTTTTACG CAACCTCTGTAGTG	3'-BHQ1
compA1-22bp(A3)	GCCCACACTTTTTTTTTTTTTTTTTTTTTTTTTTTGACAGACG CAACCTCTGTAGTG	3'-BHQ1
compA1-29bp(A3)	GCCCACACTTTTTTTTTTTTTTTTTTTAACGTGGGACAGAC GCAACCTCTGTAGTG	3'-BHQ1

References

1. S. M. Douglas, A. H. Marblestone, S. Teerapittayanon, A. Vazquez, G. M. Church and W. M. Shih, *Nucleic Acids Res.*, 2009, **37**, 5001-5006.
2. B. E. Snodin, F. Randisi, M. Mosayebi, P. Šulc, J. S. Schreck, F. Romano, T. E. Ouldridge, R. Tsukanov, E. Nir, A. A. Louis and J. P. Doye, *J. Chem. Phys.*, 2015, **142**, 234901.
3. P. Šulc, F. Romano, T. E. Ouldridge, L. Rovigatti, J. P. Doye and A. A. Louis, *J. Chem. Phys.*, 2012, **137**, 135101.
4. T. E. Ouldridge, A. A. Louis and J. P. Doye, *J. Chem. Phys.*, 2011, **134**, 085101.
5. C. Maffeo and A. Aksimentiev, *Nucleic Acids Res.*, 2020, **48**, 5135-5146.
6. A. Suma, E. Poppleton, M. Matthies, P. Šulc, F. Romano, A. A. Louis, J. P. K. Doye, C. Micheletti and L. Rovigatti, *J. Comput. Chem.*, 2019, **40**, 2586-2595.
7. W. Humphrey, A. Dalke and K. Schulten, *J. Mol. Graphics*, 1996, **14**, 33-38, 27-38.